Simulations of an Electromagnetic Microsystem Used in Biomedical Applications

T. Creutzburg and H. H. Gatzen
Institute for Microtechnology, Leibniz Universität Hannover, Garbsen, Germany

Abstract— Simulations of an electromagnetic microsystem intended to be used in a microactuator which serves as an ear implant to overcome amblyacousia were conducted. Using the ANSYS^{TM} simulation software, the design and optimization of the electromagnetic microsystem were accomplished by Finite Element Method (FEM) analyses. The design process contained 2-D and 3-D simulations. 2-D simulations served as parametric studies of the system. Afterwards, a 3-D simulation was carried out to fine-tune the results of the 2-D simulation. Comparing the 3-D with the 2-D simulation, the resulting force-air gap data were very close. With respect to the simulations, the designed electromagnetic system fulfils the requirements to drive the microactuator.

1. INTRODUCTION

In the year 2001, the World Health Organization (WHO) reported that there were about 250 million people worldwide suffering from a disabling hearing impairment. About 70 million of those people lived in Europe and 28 million in the USA [1]. The therapy for hearing impaired patients reaches from simple-plug in to implantable active hearing aids as well as Total or Partial Ossicular Replacement Prostheses (TORP/PORP), depending basically on the type and severity of the hearing loss [2]. For implantable active hearing aids, there are alternatives: middle and inner ear implants as well as Bone Anchored Hearing Aids (BAHA's). On the market of middle ear implants, several conventionally fabricated hearing implants are available [3]. The goal of this work was to design an electromagnetic device for a hearing implant fabricated by Micro Electromechanical Systems (MEMS) technology. A main advantage of such an approach is the batch fabrication, reducing the costs for the system [4]. The desired hearing implant located at the round window is intended to stimulate the perilymph using a plunger. A schematic view of the ear implant is shown in Fig. 1(a).

By applying the electromagnetic principle, different microactuators like a bi-stable optical microswitch [5] or an integrated second stage microactuator for a hard disk recording head [6] were designed and fabricated at the Institute for Microtechnology (imt). A proven approach for the design of such microsystems is to create a Finite Element Method (FEM) model for these systems and simulate their behavior when excited [7]. Applying this approach, the electromagnetic device used in the hearing implant was designed by 2-D and 3-D electromagnetic simulations. Design limitations were given by the microtechnological fabrication and the maximum dimensions of the hearing implant resulting from the physiological restrictions in the middle ear and the cochlea.

The electromagnetic device consists of a microcoil system and soft-magnetic flux guides. Basically, the structure corresponds to a pot magnet. The circular-shaped soft-magnetic lower core and inner pole, the flux closure (fixed to a membrane) as well as the ring-shaped outer pole consist

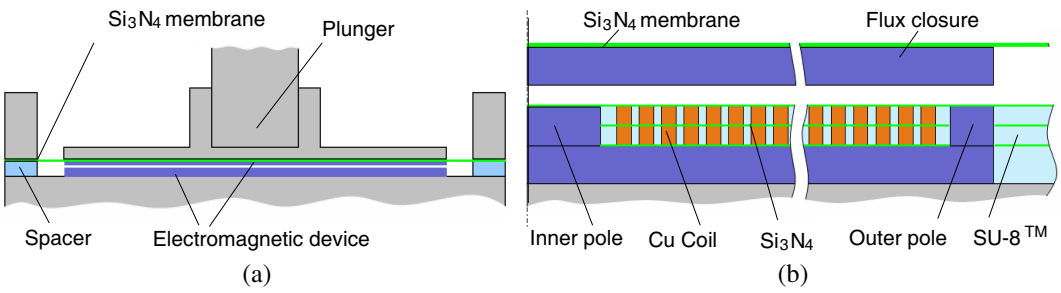

Figure 1: Schematic representation of the electromagnetic inner ear implant: (a) Cross section of the ear implant; (b) Cross section of the electromagnetic device.

of NiFe45/55. The Cu coil system is located above the lower core between inner and outer pole underneath the flux closure. The system is embedded in the photosensitive epoxy SU-8^{TM}. Si_3N_4 is used as an insulator between the coil layers. The system is shown in Fig. 1(b).

2. REQUIREMENTS OF THE MICROACTUATOR

The requirement the electromagnetic device has to fulfill is to supply the force necessary to stimulate the perilymph through the round window. This force was determined by simulating the ear implant under the load of the cochlea. For carrying out the simulations, the cochlea was modeled as a damper and the system's behavior in a frequency range of 100 Hz to 10 kHz was simulated. The minimum force the electromagnetic device has to provide at an air gap of 10 µm is about 11 mN.

Due to the maximal dimensions of the implant and the desired resonant frequency the system has to reach, a diameter of 1,750 µm was chosen for the electromagnetic device. This diameter was determined by simulating the mechanical parts of the implant using different diameters of the flux closure until the desired resonant frequency was reached. These simulations are discussed in [8].

3. 2-D SIMULATIONS

Based on the selected system diameter of 1,750 µm, four different electromagnetic systems were modelled using the ANSYS^{TM} Parametric Design Language (APDL). By combing ANSYS^{TM} rectangle primitives, the structures of the systems, i.e., the flux guides and the coil system, were created considering the rotational symmetry of the systems. Overlapping the structures with a half circle representing the surrounding air resulted in the final axially symmetric model. The SU8^{TM} embedding and the Si_3N_4 insulations were neglected because both materials behave like air in an electromagnetic simulation. Using the elements Infin110 and Plane53, the models were meshed applying the appropriate material properties. These material properties were the relative permeability for air, the relative permeability and resistivity for Cu as well as a non-linear *BH*-loop and the respective coercive force for NiFe45/55. Infin110 elements were used to mesh the outer element layer of the surrounding air, modelling the effect of far-field decay. Additionally, the outer nodes were selected and flagged as infinite surface. Plane53 elements were applied to mesh the rest of the model. In the following, a component was created containing the elements of the flux closure. Using the macro FMAGBC, Maxwell and virtual work force boundary conditions were applied to this component. The excitation was carried out by providing current density loads to the areas of the coil system. A meshed model of one system is shown in Fig. 2.

The steps described were carried out for each of the four systems considered. The four systems were modeled step by step, changing the properties of the initial system 1 until a configuration matched the requirements of the ear implant. By varying the air gap between 2.5 µm and 10 µm and simulating the systems, the force depending on the respective air gap was analyzed. The main properties of the systems are given in Table 1.

The first system investigated consisted of a 10 µm thick lower core and flux closure, an inner

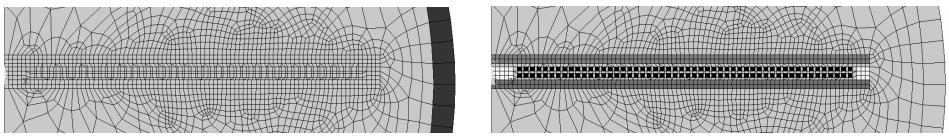

(a) (b)

Figure 2: 2-D FEM simulation: (a) Mesh showing element types; (b) Mesh showing material types.

Table 1: Main properties of the simulated systems.

System	Number of the coil layers	Number of the coil windings	Height of the flux guides	Diameter of the inner pole	Width of the outer pole	Force at 10 µm air gap
1	1	54	10 µm	50 µm	20 µm	2.4 mN
2	2	108	10 µm	50 µm	20 µm	4.0 mN
3	2	108	20 µm	50 µm	20 µm	9.6 mN
4	2	104	20 µm	100 µm	30 µm	11.2 mN

pole with a diameter of 50 µm, an outer pole with a width of 20 µm, and a single-layer coil. The system did not match the requirements, reaching a maximum force of only 2.4 mN for an air gap of 10 µm. The second system analyzed was a double-layer coil version of the first system. The intention for the doubling was to increase the flux density and the corresponding attractive force. Nevertheless, with a maximum of 4.0 mN, the system did not supply the desired force either. In a third attempt, the height of the lower core and the flux closure was changed to 20 µm. Increasing the height of these flux guides, the used *BH*-loop for NiFe45/55 had to be changed. In case of a thicker layer, the relative permeability μ_r reduces, but the cross sectional area of the flux guide increases, thus decreasing the reluctance. As a result, an increase in the flux density and the corresponding attractive force could be assumed. The simulation provided a force of 9.6 mN at an air gap of 10 µm. Nevertheless, parts of the flux guides were magnetically saturated. For that reason, the number of coil windings was reduced and the diameter of the inner pole and the width of the outer pole were increased to 100 µm and 30 µm, respectively. This approach increased the area featuring the height of the attractive force. The system provided a force of 11.2 mN matching the requirements. The results of the simulations of each electromagnetic device modeled are shown in Fig. 3.

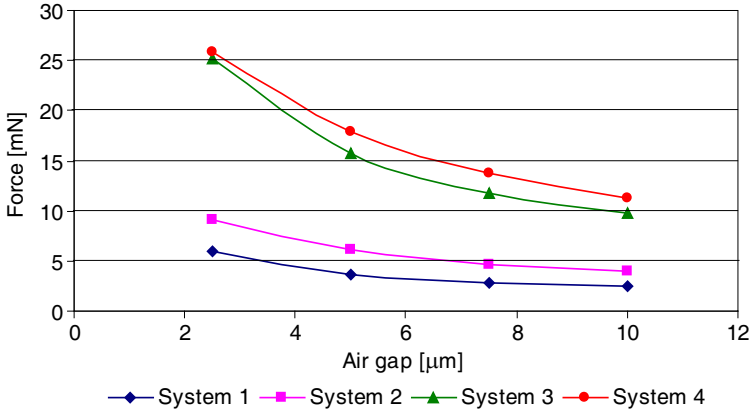

Figure 3: 2-D FEM simulation results for the forces of systems 1 through 4 as a function of the air gap.

4. 3-D SIMULATION

System 4 was modeled in 3-D to confirm the results of the 2-D simulation. The modeling procedure was carried out like in the 2-D simulation. The geometry model was generated using ANSYS^{TM} primitives. The coil system was chosen as a stranded coil, defining the properties with a real constant. The surrounding air was represented by an overlapping sphere. The meshing of the model was carried out using Solid97, Infin111, and Circu124 elements. Infin111 elements were used for the outer layer of the modeled air acting like Infin110 elements in the 2-D simulation. The creation of the Infin111 elements was realized by selecting the outer area of the already meshed surrounding air and extruding the existing elements by one element. After that, all outer nodes were selected and flagged as infinite surface. Since Solid97 elements were used, a *BH*-loop could not be used to define the magnetic properties of the NiFe45/55. Instead, the *BH*-loop applied in the 2-D simulations was linearized in three sections and the respective relative permeability was used for the 3-D simulation. The excitation of the stranded coil was done by coupling the coil to a Circu124 element. Initially, the elements of the meshed stranded coil were selected and coupled in relation to current and electromotive force. In the next step, two single nodes were created outside the model. Afterwards, a Circu124 coupling element was generated by the use of the two nodes and a third node of the stranded coil. After applying the boundary conditions voltage (0 V) and current (0.1 A) to the nodes of the coupling element, the 3-D model was simulated. Changing the air gap, the force depending on the respective air gap was analyzed.

5. COMPARISON OF 2-D AND 3-D SIMULATIONS

In Fig. 4, the flux density distribution in the flux closure of the 2-D and 3-D models is shown. The result of the 2-D simulation is shown as an axially symmetric expansion to get a 3-D view for a better comparison. Fig. 5 presents the forces depending on the respective air gap for the 2-D

and 3-D simulations. Comparing the 3-D with the 2-D simulation, the flux density distributions are quite similar. This is due to the fact that there is a good agreement between 2-D and 3-D simulations for axially symmetrical structures.

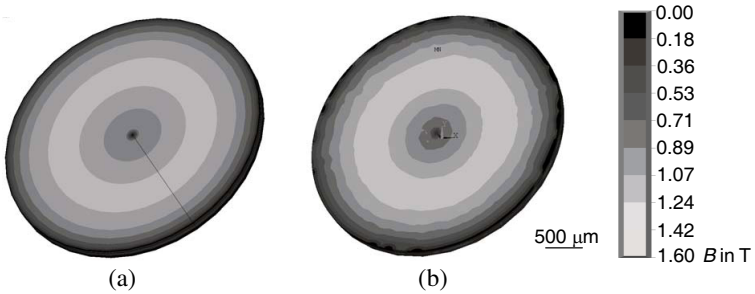

Figure 4: Flux density distribution of system 4: (a) 2-D simulation results; (b) 3-D simulation results.

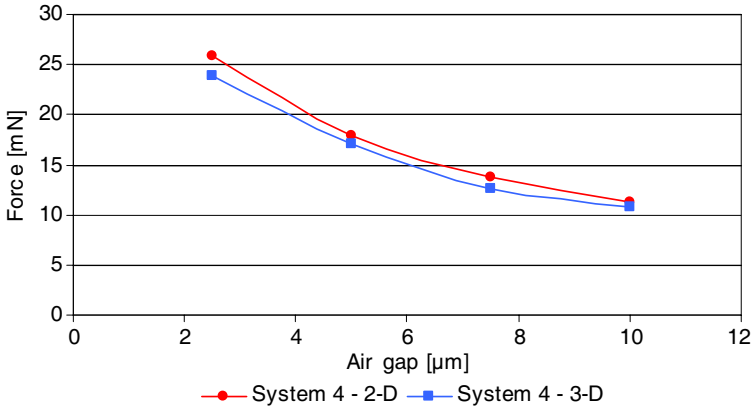

Figure 5: Simulated forces of system 4 — comparison between the 2-D and 3-D models.

6. CONCLUSIONS

Using 2-D FEM-simulations, an electromagnetic device could be designed which fulfills the requirements to drive the ear implant. By comparing the 2-D simulation with a 3-D simulation, the results of the 2-D simulation could be fine-tuned. Thus, performing 2-D simulations are a suitable way to design such an electromagnetic device due to the fact that less modelling and simulation time is needed in the 2-D simulation.

ACKNOWLEDGMENT

This research is sponsored by the DFG (German Research Foundation) within the program "Inner Ear Microtransducer for the Stimulation of the Perilymph in case of Amblyacousia".

REFERENCES

1. Shield, B., "Evaluation of the social and economic costs of hearing impairment," A Report for Hear-It, 2006
2. Wintermantel, E. and S.-W. Ha, *Medizintechnik*, Berlin Heidelberg, Springer, 2009.
3. Haynes, D. S., J. A. Young, G. B. Wanna, and M. E. Glasscock, "Middle ear implantable hearing devices: An overview," *Trends in Amplification*, Vol. 13, No. 3, 206–214, 2009.
4. Schomburg, W. K., R. Ahrens, W. Bacher, C. Goll, S. Meinzer, and A. Quinte, "Amanda-low-cost production of microfluidic devices," *Sensors and Actuators A: Physical*, Vol. 70, No. 1–2, 153–158, 1998.
5. Gatzen, H. H., E. Obermeier, T. Kohlmeier, T. Budde, H. D. Ngo, B. Mukhopadhyay, and M. Farr, "An electromagnetically actuated bi-stable MEMS optical Microswitch," *12th International Conference on Transducers, Solid-state Sensors, Actuators and Microsystems*, 1514–1517, Boston, USA, June 2003.

6. Dinulovic, D., H. Saalfeld, Z. Celinski, S. B. Field, and H. H. Gatzen, "Integrated electromagnetic second stage microactuator for a hard disk recording head," *IEEE Transactions on Magnetics*, Vol. 44, No. 11, Part 2, 3730–3733, 2008.
7. Dinulovic, D. and H. H. Gatzen, "An approach for simulating magnetic microactuators," *International Conference on Thermal, Mechanical and Multi-physics Simulation and Experiments*, 1–4, Freiburg, Germany, April 2008.
8. Creutzburg, T. and H. H. Gatzen, "Design of a microactuator for the stimulation of the perilymph," *International Conference on Thermal, Mechanical and Multi-physics Simulation and Experiments*, Bordeaux, France, April 2010, (submitted).